Organic Geochemistry 142 (2020) 103995

Contents lists available at ScienceDirect

Organic Geochemistry

journal homepage: www.elsevier.com/locate/orggeochem

An automated solid phase extraction procedure for lipid biomarker purification and stable isotope analysis

Oliver Rach [a,*], Xennophone Hadeen [a,b], Dirk Sachse [a]

[a] GFZ – German Research Centre for Geosciences, Section 4.6, Geomorphology, Organic Surface Geochemistry Lab, Telegrafenberg, 14473 Potsdam, Germany
[b] School of Earth and Environmental Science, James Cook University, Cairns, Queensland, Australia

ARTICLE INFO

Article history:
Received 28 October 2019
Received in revised form 19 February 2020
Accepted 21 February 2020
Available online 25 February 2020

Keywords:
Compound separation
Fatty acids
n-Alkanes
Hydrocarbon
Stable hydrogen isotopes

ABSTRACT

Effective recovery and high purity of lipid biomarkers are essential for compound-specific stable isotope analysis in a variety of fields ranging from hydrocarbon research, paleoclimatology, food and drug analysis and medicine. Solid-phase extraction (SPE) is the most common method for purifying organic compounds from complex mixtures. SPE constitutes the most labor-intensive part of laboratory work often limiting the number of samples that can be analyzed. Reliable, easy-to-use, automated methods could increase sample throughput as well as reproducibility. Here we introduce such a method using a Gilson ASPEC GX-271 system and test the separation quality, reproducibility, and efficiency in comparison to a classical manual SPE lipid purification procedure. Using multiple extractions of the same natural soil sample we show that the automated SPE is comparable in overall quality and slightly superior in reproducibility to a manual SPE. We demonstrate that stable hydrogen isotope measurements of *n*-alkanes purified using an automated SPE extraction showed significantly lower standard errors. Furthermore, the unattended operation of the system eases the purification of large sample sets. Generally, the automated SPE using the Gilson ASPEC GX-271 for lipid biomarker separation provides qualitatively and quantitatively accurate and reproducible results with more efficient purification of compounds than the manual method.

1. Introduction

Effective recovery and reliable lipid biomarker identification, as well as quantification, is the essential work step in disciplines ranging from hydrocarbon exploration, forensics, food control, pharmaceutical analysis to paleoclimatology. Environmental samples, such as plant and animal products, soils and sediments, contain a broad spectrum of different organic molecules. Reliable gas- or liquid chromatographic analysis of these compounds often requires separation into different fractions of similar polarity. A classical and often used separation method is solid-phase extraction (SPE) (Zelles and Bai, 1993; Stout et al., 2001; Poole, 2003; Telepchak et al., 2004; Sessions, 2006; Xu and Lee, 2008; Hoffmann et al., 2013), which has become a valuable sample purification step in modern organic geochemistry (Sessions, 2006; Vogts et al., 2009; McInerney et al., 2011; Romero and Feakins, 2011; Atwood and Sachs, 2012; Ladd and Sachs, 2012; Wohlfarth et al., 2018). In particular, the trend towards temporally and spatially highly resolved compound-specific stable isotope datasets in paleoenvironmental analysis (Rach et al., 2014; Gamarra et al., 2016; Nelson et al., 2017; Curtin et al., 2019; Feakins et al., 2019; Zhou et al., 2019) requires baseline separated peaks within the chromatograms (i.e. no co-elution of different compounds) to avoid misinterpretations (Wang and Sessions, 2008).

The classic method for compound purification is solid-phase extraction (SPE). Typically, a sample extract is applied to a stationary phase (a solid sorbent in a column, often silica gel) which is then rinsed with a mobile phase (a solvent dissolving the organic compounds of interest from the extract) (Telepchak et al., 2004). By rinsing the column with solvents of increasing polarity (sometimes referred to as 'normal phase'), separation is achieved as more polar molecules go into solution and elute stepwise from the column, where they can be collected. This method is well established but remains often a largely manual task. Even in today's laboratories with increasing automation the number of samples is limited. A few automated approaches exist with specialized equipment (i.e. Medium Pressure Liquid Chromatography systems (MPLC) (Radke et al., 1980), or in industrial applications of SPE (drug purification, environmental trace analysis), but these have limitations. They

* Corresponding author.
E-mail address: oliver.rach@gfz-potsdam.de (O. Rach).

https://doi.org/10.1016/j.orggeochem.2020.103995
0146-6380/

apply only to simple compound mixtures (i.e. pharmaceutical applications) and/or still require user attendance in the case of MPLC.

In this study, we test the applicability of a commercially available automated SPE (aSPE) system (Gilson.com, 2019), frequently used in clinical, forensic, doping, food, and environmental applications with water as a mobile phase. We modified the system for lipid biomarker separation with an organic solvent as the mobile phase.

Specifically, we compared the separation of the same soil lipid extract by manual SPE (mSPE) to a fully automated Gilson ASPEC GX-271 aSPE system. We performed the classical separation of a total lipid extract (TLE) into three fractions (F1 – low polarity, F2 – medium polarity and F3 – high polarity). While both methods rely on the same principle of separation, they are characterized by slight differences in liquid handling and the elution principle (negative pressure for mSPE vs overpressure for aSPE). We evaluate the advantages and disadvantages of aSPE in contrast to the classic mSPE application for lipid biomarker purification. To compare purification quality and reproducibility, we tested both procedures on four different amounts of the same TLE (15 mg, 20 mg, 25 mg, and 30 mg) in triplicate with both methods. Particularly, we aimed to evaluate the analytical accuracy (i.e. separation quality, concentrations of major compounds and reproducibility) of this aSPE system during lipid biomarker purification but also for more general conditions (e.g., the time needed per sample). In addition, we tested the reliability of both SPE methods for compound-specific hydrogen isotope analysis of the low polarity fraction.

2. Sample collection, extraction and pre-processing

The sample soil material (upper 0–3 cm of topsoil below the litter horizon) was collected on the campus of the German Research Centre for Geosciences (GFZ) in Potsdam (Germany) under an oak tree (52° 22′ 59.68″ N, 13° 03′ 48.02″ E, 79 m asl) on the fringe of a natural forest. The collected soil was dried in a porcelain bowl for 5 days at 50 °C in a drying cabinet and subsequently sieved (1 mm sieve) to remove particles bigger than 1 mm (e.g., leaf parts, stones, large roots, wood pieces). In total 818 g of dry soil was then homogenized to a fine powder by hand using a porcelain mortar. Organic matter was then extracted from 300 g of dry soil using a Dionex Accelerated Solvent Extraction system (ASE 350, Thermofisher Scientific) with dichloromethane (DCM):methanol (MeOH) mixture (9:1, v/v) at 100 °C, 103 bar pressure and two extraction cycles (20 min static time). The resulting total lipid extract (TLE) was collected in a combusted glass vial. The solvent mixture was completely evaporated under a stream of nitrogen and resulting in TLE dry weight (1.92 g). Afterward, the TLE was separated into four different aliquots of different lipid concentrations (15 mg, 20 mg, 25 mg, and 30 mg TLE respectively) (Fig. 1). For this purpose, the total TLE was dissolved in 50 ml DCM:MeOH (9:1, v/v) mixture and an aliquot respective amount (0.39 ml, 0.52 ml, 0.65 ml, and 0.78 ml) was transferred into 2 ml vials with a conical bottom structure to ensure a complete transfer of the vial content to the column during the automated SPE. Each of these aliquots was replicated in sextet resulting in 24 samples (Fig. 1). Internal standards (5α-androstane (10 μg), 5α-androstan-3β-ol (30 μg) and erucic acid (30 μg)) were added to all samples. The samples were evaporated under a stream of nitrogen. Finally, each sample was dissolved in 1 ml *n*-hexane and placed on a shaking table for 45 min. Three replicates of each TLE aliquot were processed in a total of three manual SPE separations (mSPE). Whereas the other three replicates were separated in the automated SPE system (aSPE) (Fig. 1).

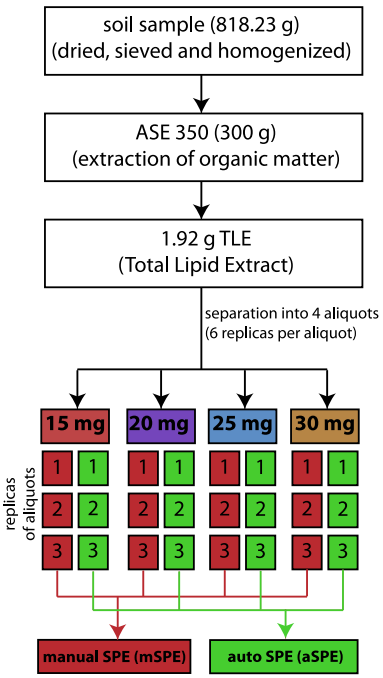

Fig. 1. Sample extraction and preparation. Separation of the sample into four aliquots and respective replicas for mSPE and aSPE.

2.1. SPE preparation

For both methods, we prepared in total 42 identical glass columns of 6 ml total volume filled with 2.25 g silica gel (pore size 60 Å, 230–400 mesh particle size) sealed with two glass fiber filters below and on top. All columns were filled in a temperature-controlled laboratory environment with freshly combusted (450 °C) silica gel. After cooling to room temperature, columns were immediately rinsed with 18 ml of acetone, DCM and *n*-hexane (to remove possible organic contaminations from the silica gel) and stored in a desiccator to prevent moisture absorption. Both mSPE (Fig. 2B) and aSPE (Fig. 2A) extractions resulted in three fractions. In both cases, fractions were eluted from a silica gel column according to their polarity using different solvent mixtures (F1 – *n*-hexane for elution of *n*-alkanes, F2 – *n*-hexane:DCM in a ratio of 1:1 (v/v) for elution of ketones, F3 – DCM:MeOH (1:1, v/v) for elution of fatty acids and alcohols).

2.1.1. Manual SPE (mSPE)

Manual SPE was conducted by one experienced technician on an SPE manifold vacuum-block, holding a maximum of 12 columns each. The procedure is based on established methods (Sessions, 2006) with modifications outlined below. Prepared SPE columns were installed on top of stainless-steel needles with valves. Collection tubes (18 × 100 mm) were placed in the chamber below to collect the effluent. A vacuum port with a gauge can be utilized to control the vacuum in the chamber, permitting the control of the liquid flow rate of the sample fractions when the flow of the effluent is very low or static.

Before mSPE was initiated, columns, needles, and valves were flushed with *n*-hexane. The TLEs (dissolved in *n*-hexane) was stirred for 10 min in a centrifuge and transferred via glass pipettes to SPE columns. Fraction F1 was eluted with 14 ml of *n*-hexane and collected in a reaction tube. Once the *n*-hexane has passed through the column, the valve was closed and the collection vials in the chamber were replaced with collection vials for fraction F2. The TLE vial was additionally rinsed with 1 ml of *n*-hexane:DCM (1:1,

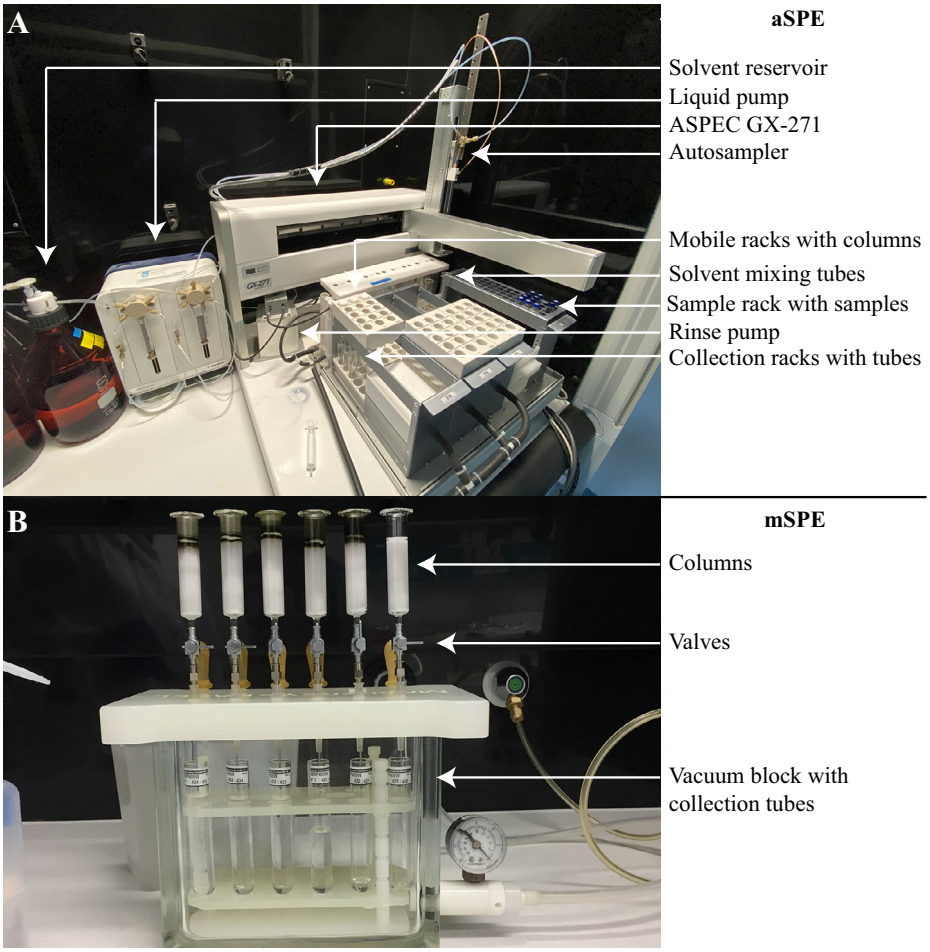

Fig. 2. Setup of compared SPE methods. (A) aSPE, (B) mSPE.

v/v) mixture which was also transferred to the SPE column, to ensure that higher polarity molecules that may not have been dissolved in the initial *n*-hexane step are recovered. In the following step, 13 ml of *n*-hexane:DCM (1:1) mixture was used for the elution of fraction F2 from the column. Subsequently, the collection vials were replaced, the TLE vial was rinsed again with 1 ml mixture of the next eluent (DCM:methanol (1:1, v/v)) and 13 ml of a DCM:methanol (1:1, v/v) mixture was applied for elution and collection of fraction F3.

mSPE was conducted in triplicate with the same four samples (15 mg TLE, 20 mg TLE, 25 mg TLE, 30 mg TLE) and one blank column for assessing reproducibility. Processing time for mSPE in this configuration depends on the experience of the user and sample type. In our case, the meantime for a 4-sample run (+1 blank column) with 3 fractions eluted per sample was 62 min.

2.1.2. Automated SPE (aSPE)

For aSPE we used an Aspec GX-271 system (Gilson, Inc.) in combination with a two-syringe liquid pump (verity 4260) and one additional peristaltic pump (for outside needle rinse). The system is controlled by Trilution LH software (Gilson, Inc). The liquid pump is connected to two 2.5 l reservoir bottles of *n*-hexane and DCM. The Aspec GX-271 bed layout consists of in total nine modules: one four-bottle rack for 650 ml glass bottles (item code (ic): 123 GX-271), three collection racks (ic: collect 376), three mobile racks (ic: DEC 376 mobile rack), one tube rack for 44 tubes (size: 18 × 100 mm) (ic: 22) and one vial rack for 60 vials (size: 2 ml) (ic: 330).

We used a commercially available system of the Aspec GX-271 platform with slight custom modifications to the collection and mobile racks for an application with organic solvents. The diameter and depth of the tube positions on the collection racks were slightly increased to support larger 18 × 100 mm collection vials (standard: 15 × 85 mm) to increase the total collection volume per fraction. Also, the holes which hold the columns within the mobile racks were slightly widened in diameter to fit 6 ml glass columns (standard: plastic columns). Additionally, the standard plastic column plugs (pressure caps) were replaced by self-designed and produced solvent-resistant PTFE caps to avoid possible sample contamination during elution.

The aSPE procedure for separation of one TLE into three fractions of increasing polarity was based on the mSPE steps (Section 2.1.1) and consists of 26 operational steps (predefined software functions) (Fig. 3). This fully automated procedure took 92 min per sample. In the current bed layout and with the number of target fractions (three) the machine processes nine subsequent samples. During the separation of the test samples, we ran a blank before and after each sample (blank – sample alternation) to assess possible cross-contamination during sample switching. The aSPE was run in this configuration three times on the same samples (i.e. replicates) for assessment of reproducibility.

2.2. Post SPE handling

All mSPE and aSPE fractions (F1, F2, and F3) were treated the same in subsequent steps. The fractions were transferred into 2 ml

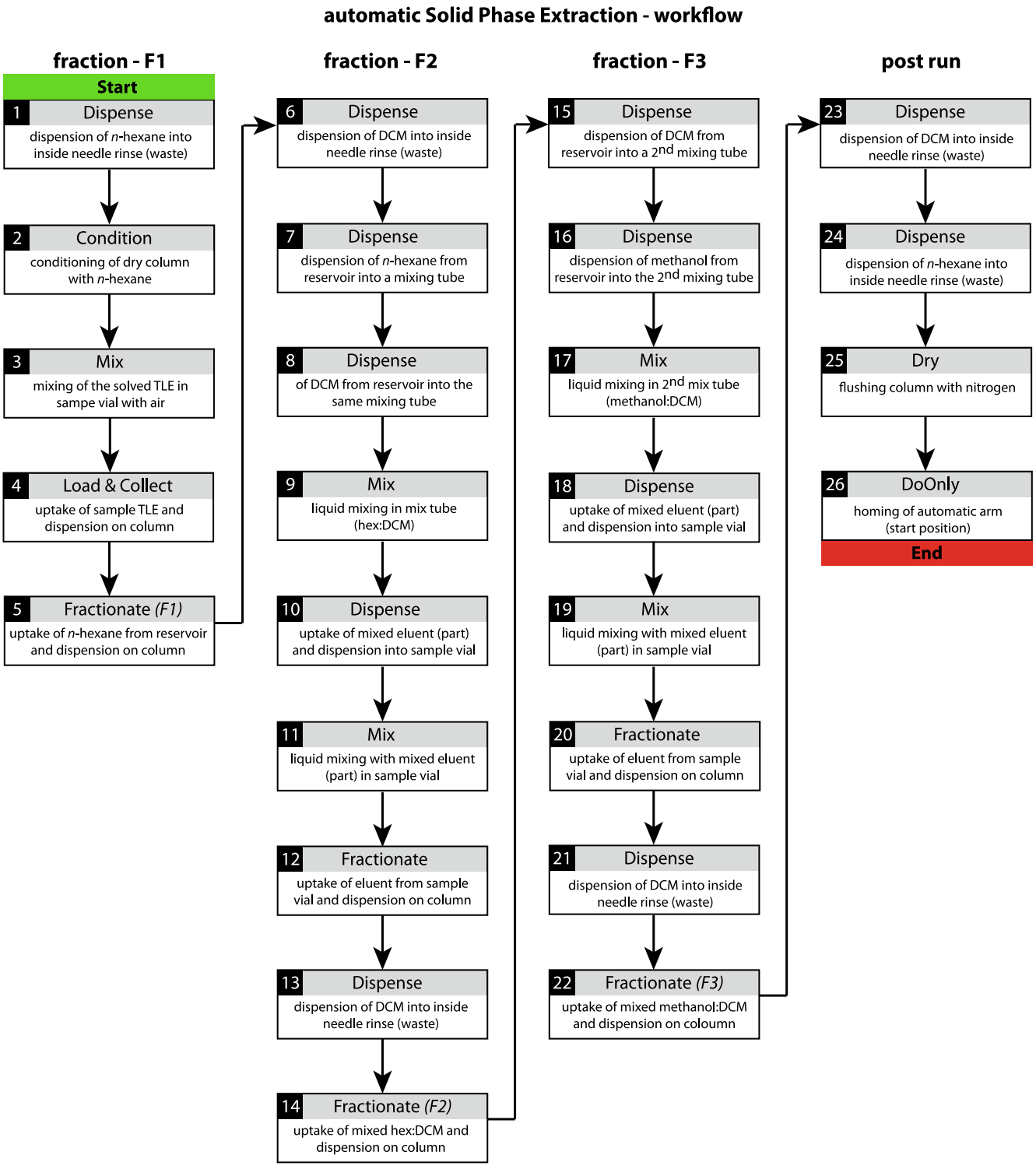

Fig. 3. aSPE functional workflow including a detailed description of work steps and functions during aSPE.

vials and dissolved in 400 μl of solvent (F1 in *n*-hexane, F2 and F3 in DCM). F3 was derivatized using 50 μl of BSTFA before analysis. For compound identification and quantification, all samples were analyzed in triplicate on an Agilent 7890 gas chromatograph (GC) coupled to a flame ionization detector (FID) and Agilent 5975 single-quad mass spectrometer (MS). The GC was equipped with a 30 m Agilent DB-5MS UI column (0.25 μm film thickness, 25 mm diameter). Additionally, three replicates of external standards (5α-androstane (10 μg), 5α-androstan-3β-ol (30 μg) and erucic acid (30 μg)) were measured in 400 μl of solvent for a reliable compound quantification of alkanes, aldehydes, ketones and fatty acids (FA). The resulting peak areas of all three replicate measurements of the external standards, as well as the samples, were used to calculate a mean area and used for compound quantification. Sample results were normalized to their initial TLE weight and are reported as μg/g TLE with the corresponding standard error of the mean (SE).

Compound-specific stable hydrogen isotope measurements (δ^2H) were conducted on *n*-alkanes from the F1 fractions using a Trace GC 1310 (ThermoFisher Scientific) connected to Delta V plus Isotope Ratio Mass Spectrometer (IRMS) (ThermoFisher Scientific).

The GC was equipped with an Agilent DB-5MS UI column (0.25 μm film thickness, 25 mm diameter). *n*-Alkane δ^2H values were determined by duplicate measurements. An *n*-alkane standard-mix A6 (*n*-C_{16} to *n*-C_{30}) with known δ^2H values obtained from A. Schimmelmann (Indiana University) was measured before and after the samples and used for correction and transfer to the VSMOW scale. During the 2-days measurement period the $H3^+$ factor was stable at 3.09 ± 0.02 mV.

2.3. Statistical processing

Significance of differences was tested through the *t*-test and respective *p*-values (95% confidence interval) were calculated using Aabel software. For determination of the respective error ranges of compound amounts and isotope values, the standard deviation (SD), as well as the standard error of the mean (SE), were calculated. Error ranges in the text and figures show the standard error of the mean from replicate measurements. Since this study compares mainly differences between mean values of three replicate measurements from two different purification methods it is appropriate to show error ranges as the standard error of the mean instead of the standard deviation. For comparison, in Tables 1 and 2 we also present the standard deviations. The error range of concentrations is considered until 0.01 μg/g (10 ng/g). Errors below 0.01 μg/g (10 ng/g) are stated as ± 0.00 μg/g.

3. Results

3.1. Manual SPE (mSPE)

One blank column was produced in each of the three mSPE extraction runs. No compounds were detected in the blank fractions.

3.1.1. Manual SPE Fraction 1

The first SPE fraction (F1 – low polarity) contained *n*-alkanes from *n*-C_{25} to *n*-C_{33}, a typical distribution for mid-latitude forest soils. The concentrations ranged from 0.13 ± 0.00 μg/g (mean ± standard error of the mean) to 0.89 ± 0.01 μg/g. From all identified *n*-alkanes *n*-C_{33} showed the lowest concentrations whereas *n*-C_{27} was most abundant (Fig. 4A, B, C). Generally, the *n*-alkane concentrations from mSPE extracts ($F1_{mSPE}$) showed small variations for different TLE sample weights. The 15 mg TLE sample ($F1_{(15)mSPE}$) contained the highest individual *n*-alkane concentrations (range from 0.17 ± 0.00 μg/g TLE to 0.89 ± 0.01 μg/g TLE for the different *n*-alkane homologues) (Fig. 5A, Table 1). For $F1_{(20)mSPE}$, $F1_{(25)mSPE}$ and $F1_{(30)mSPE}$ the *n*-alkanes showed concentrations in a range between 0.13 ± 0.00 μg/ g TLE and 0.74 ± 0.03 μg/g TLE. However, these variations were mostly within the range of the SE (Fig. 5A, Table 1). The *n*-alkane mean concentration (overall manual processed TLE samples) was for *n*-C_{25} 0.19 ± 0.01 μg/g TLE, for *n*-C_{27} 0.56 ± 0.03 μg/g TLE, for *n*-C_{29} 0.76 ± 0.04 μg/g TLE, for *n*-C_{31} 0.44 ± 0.03 μg/g TLE and for *n*-C_{33} 0.15 ± 0.01 μg/g TLE (Fig. 6A).

In the 15 mg, 20 mg and 25 mg TLE aliquot of the $F1_{mSPE}$ fraction (only 1st replicate) and in the 30 mg TLE aliquot of the $F2_{mSPE}$ fraction (only 2nd replicate) we additionally identified the unsaturated compounds 1,2-benzacenaphthene and pyrene (Fig. 4B) in amounts between 0.05 μg/g TLE and 0.20 μg/g TLE (no SE is reported because compounds were not present in all replicates). The lowest concentration was detected in $F1_{(25)mSPE}$ whereas the highest concentration was measured in $F1_{(15)mSPE}$. In $F1_{(30)mSPE}$ of the 1st mSPE replicate as well as in $F1_{(15)mSPE}$, $F1_{(20)mSPE}$ and $F1_{(25)mSPE}$ of the 2nd mSPE replicate, and all the samples of the 3rd mSPE replicate. 1,2-Benzacenaphthene and pyrene were not observed in the F1 samples from the 3rd mSPE run. However, they were detected in the F2 fraction (Fig. 4A, C).

Compound-specific δ^2H measurements of *n*-C_{25} in $F1_{(15)mSPE}$, $F1_{(20)mSPE}$, $F1_{(25)mSPE}$ and $F1_{(30)mSPE}$ ranged from −164.2 ± 4.0‰ to

Table 1
Mean compound specific amounts for mSPE and aSPE samples with standard error of the mean (SE) and standard deviation (SD).

		Compound quantification											
		Manual SPE (μg/g TLE)											
Fraction	Compound	15 mg TLE	SE	SD	20 mg TLE	SE	SD	25 mg TLE	SE	SD	30 mg TLE	SE	SD
F1	*n*-C_{25}	0.22	0.01	0.01	0.18	0.01	0.02	0.17	0.01	0.01	0.18	0.00	0.01
F1	*n*-C_{27}	0.66	0.01	0.02	0.55	0.02	0.03	0.52	0.00	0.01	0.53	0.00	0.00
F1	*n*-C_{29}	0.89	0.01	0.03	0.74	0.03	0.05	0.70	0.00	0.00	0.72	0.00	0.00
F1	*n*-C_{31}	0.51	0.01	0.01	0.43	0.01	0.02	0.40	0.00	0.01	0.42	0.00	0.00
F1	*n*-C_{33}	0.17	0.00	0.00	0.14	0.00	0.01	0.13	0.00	0.00	0.14	0.00	0.00
F2	*n*-hexacosanal	1.14	0.02	0.03	0.92	0.03	0.06	0.87	0.02	0.03	0.89	0.01	0.02
F2	*n*-octacosanal	1.37	0.01	0.02	1.19	0.02	0.03	1.03	0.03	0.04	1.06	0.02	0.04
F2	*n*-triacontanal	0.80	0.00	0.00	0.69	0.01	0.01	0.60	0.02	0.03	0.62	0.01	0.02
F2	friedelan-3-one	0.44	0.25	0.43	0.29	0.16	0.28	0.06	0.06	0.11	0.77	0.40	0.70
F3	C_{16} FA	1.63	0.12	0.21	1.35	0.07	0.12	1.23	0.04	0.06	1.24	0.05	0.09
F3	C_{18} FA	0.56	0.04	0.07	0.44	0.02	0.03	0.39	0.01	0.02	0.41	0.01	0.02
F3	C_{20} FA	0.62	0.04	0.07	0.45	0.01	0.02	0.35	0.01	0.02	0.45	0.01	0.02
F3	C_{22} FA	1.35	0.11	0.20	0.90	0.03	0.05	0.66	0.02	0.04	0.84	0.03	0.05
		Automated SPE (μg/g TLE)											
Fraction	Compound	15 mg TLE	SE	SD	20 mg TLE	SE	SD	25 mg TLE	SE	SD	30 mg TLE	SE	SD
F1	*n*-C_{25}	0.22	0.01	0.01	0.19	0.01	0.01	0.18	0.01	0.01	0.19	0.01	0.02
F1	*n*-C_{27}	0.64	0.01	0.02	0.56	0.02	0.03	0.53	0.02	0.03	0.55	0.02	0.03
F1	*n*-C_{29}	0.87	0.01	0.01	0.75	0.02	0.03	0.72	0.02	0.03	0.74	0.02	0.03
F1	*n*-C_{31}	0.49	0.00	0.01	0.43	0.01	0.01	0.42	0.01	0.02	0.42	0.01	0.02
F1	*n*-C_{33}	0.17	0.00	0.00	0.15	0.00	0.01	0.14	0.00	0.01	0.14	0.00	0.01
F2	*n*-hexacosanal	1.16	0.08	0.14	1.04	0.09	0.16	0.99	0.07	0.13	1.01	0.04	0.08
F2	*n*-octacosanal	1.35	0.11	0.19	1.18	0.11	0.20	1.11	0.10	0.18	1.13	0.06	0.11
F2	*n*-triacontanal	0.79	0.08	0.13	0.69	0.07	0.13	0.65	0.07	0.13	0.66	0.06	0.10
F2	friedelan-3-one	2.37	0.07	0.11	2.11	0.11	0.18	1.96	0.07	0.12	2.01	0.00	0.01
F3	C_{16} FA	1.66	0.10	0.17	1.31	0.04	0.07	1.24	0.08	0.13	1.30	0.06	0.10
F3	C_{18} FA	0.55	0.03	0.06	0.42	0.01	0.02	0.39	0.02	0.04	0.41	0.02	0.04
F3	C_{20} FA	0.63	0.07	0.12	0.45	0.05	0.08	0.43	0.05	0.10	0.44	0.07	0.12
F3	C_{22} FA	1.37	0.21	0.36	0.95	0.14	0.24	0.93	0.18	0.31	0.89	0.21	0.36

Table 2
Compound specific *n*-alkane mean δ^2H values for mSPE and aSPE samples with standard error of the mean (SE) and standard deviation (SD).

		Compound-specific δ^2H Manual SPE (‰)											
Fraction	Compound	15 mg TLE	SE	SD	20 mg TLE	SE	SD	25 mg TLE	SE	SD	30 mg TLE	SE	SD
F1	*n*-C_{25}	−164.2	4.0	7.0	−165.9	1.8	3.1	−166.6	2.5	4.3	−165.7	3.9	6.8
F1	*n*-C_{27}	−169.4	0.8	1.4	−168.6	0.6	1.0	−168.3	1.5	2.6	−167.9	1.8	3.1
F1	*n*-C_{29}	−163.3	1.0	1.7	−162.3	0.8	1.4	−161.2	2.1	3.6	−162.0	1.2	2.1
F1	*n*-C_{31}	−172.3	1.1	1.9	−171.6	0.5	0.8	−170.0	2.6	4.4	−171.1	1.4	2.4
F1	*n*-C_{33}	−159.9	2.2	3.8	−159.7	1.4	2.4	−158.2	2.5	4.4	−159.5	1.9	3.3
		Automated SPE (‰)											
Fraction	Compound	15 mg TLE	SE	SD	20 mg TLE	SE	SD	25 mg TLE	SE	SD	30 mg TLE	SE	SD
F1	*n*-C_{25}	−158.7	1.6	2.7	−156.6	0.6	1.0	−157.3	1.1	2.0	−158.3	1.6	2.7
F1	*n*-C_{27}	−169.3	0.5	0.9	−168.6	0.3	0.5	−168.4	0.6	1.0	−168.2	0.6	1.1
F1	*n*-C_{29}	−164.1	0.7	1.2	−163.1	0.5	0.9	−162.3	0.5	0.9	−162.8	0.6	1.0
F1	*n*-C_{31}	−173.3	0.4	0.7	−172.9	0.5	0.9	−172.4	0.5	1.0	−172.5	0.7	1.3
F1	*n*-C_{33}	−161.2	0.6	1.1	−160.3	0.8	1.4	−159.6	0.6	1.0	−159.3	0.8	1.3

−166.6 ± 2.5‰. For *n*-C_{27}, *n*-C_{29}, *n*-C_{31} and *n*-C_{33} the mean values were between −168.3 ± 1.5‰ and −168.6 ± 0.6‰, −161.2 ± 2.1‰ and −163.3 ± 1.0‰, −170.0 ± 2.6‰ and −172.3 ± 1.1‰, −158.2 ± 2.5‰ and −159.9 ± 2.2‰ (Table 2), respectively. The mean *n*-alkane δ^2H values averaged over all TLE amounts for *n*-C_{25}, *n*-C_{27}, *n*-C_{29}, *n*-C_{31} and *n*-C_{33} were −165.6 ± 1.4‰, −168.5 ± 0.6‰, −162.2 ± 0.6‰, −171.2 ± 0.7‰ and −159.3 ± 0.9‰, with no systematic differences observed among the different TLE concentrations.

3.1.2. Fraction 2

The second SPE fraction (F2 – medium polarity) contained several aldehyde and ketone compounds, which were not always baseline separated in the GC-FID chromatogram (Fig. 4A, B, C). Therefore, not all compounds of the second SPE fraction were quantified. We identified and quantified three different baseline-separated aldehydes as *n*-hexacosanal, *n*-octacosanal and *n*-triacontanal ($C_{26}H_{52}O$, $C_{28}H_{56}O$, $C_{30}H_{60}O$) and the ketone friedelan-3-one ($C_{30}H_{50}O$) (Fig. 4A, B, C). Similar to the *n*-alkanes in the F1 fraction, *n*-hexacosanal, *n*-octacosanal and *n*-triacontanal from the F2 fraction of mSPE samples showed concentration variations with different TLE sample weights. The $F2_{(15)mSPE}$ sample contained the highest concentration of the three aldehydes (1.14 ± 0.02 μg/g TLE, 1.37 ± 0.01 μg/g TLE, 0.80 ± 0.00 μg/g TLE) (Fig. 5B, Table 1). In $F2_{(20)mSPE}$, $F2_{(25)mSPE}$ and $F2_{(30)mSPE}$ the three aldehydes ranged in concentration between 1.19 ± 0.02 μg/g TLE and 0.60 ± 0.02 μg/g TLE, mostly within the range of the SE (Fig. 5B, Table 1). Friedelan-3-one displayed the highest concentration (0.77 ± 0.40 μg/g TLE) in the $F2_{(30)mSPE}$ sample and the lowest concentration in $F2_{(25)mSPE}$ (0.06 ± 0.06 μg/g TLE). However, for friedelan-3-one we observed an up to 25 times higher SE than for the mean SE of the three aldehydes. The respective mean concentrations (overall mSPE samples) for *n*-hexacosanal, *n*-octacosanal and *n*-triacontanal were in a range between 0.68 ± 0.04 μg/g TLE and 1.16 ± 0.08 μg/g TLE (Fig. 6B). For friedelan-3-one we measured a mean concentration of 0.39 ± 0.15 μg/g TLE.

3.1.3. Fraction 3

The third fraction (F3 – high polarity) contained mainly aliphatic alcohols and aliphatic fatty acids (FAs) as well as sterols (Fig. 4A, B, C). We identified FAs with carbon numbers from 16 (referred to as C_{16} FA) to 30 (C_{30} FA). Only short- to mid-chained FAs (C_{16} FA, C_{18} FA, C_{20} FA, and C_{22} FA) in higher concentrations were baseline separated and quantified (Fig. 4A, B, C). Longer chain FAs (e.g., C_{28} FA, C_{30} FA) eluted in a part of the chromatogram with higher background values and co-eluted with other compounds, preventing robust quantification. We note that for applications where long-chain FAs are required to be baseline separated (i.e. compound-specific stable isotope measurements (e.g., Tierney et al., 2010)) the SPE separation procedure is usually different from our procedure here (i.e. use of aminopropyl impregnated silica gel). Similar to the observations for F1 and F2, the concentration of analyzed FAs from the F3 fraction of mSPE ($F3_{mSPE}$) showed variations for different TLE sample weights, but were mostly within the SE. The highest concentrations of C_{16} FA, C_{18} FA, C_{20} FA and C_{22} FA were detected in $F3_{(15)mSPE}$ (1.63 ± 0.12 μg/g TLE, 0.56 ± 0.04 μg/g TLE, 0.62 ± 0.04 μg/g TLE and 1.35 ± 0.11 μg/g TLE, respectively) (Fig. 5C, Table 1). For $F3_{(20)mSPE}$, $F3_{(25)mSPE}$ and $F3_{(30)mSPE}$ the identified FAs showed concentrations in a range between 0.35 ± 0.01 μg/g TLE (C_{20} FA) and 1.35 ± 0.07 μg/g TLE (C_{16} FA). These variations were mostly within the range of the SE (Fig. 5C, Table 1), except for C_{20} FA and C_{22} FA in $F3_{(25)mSPE}$. The respective mean concentrations (overall manual processed TLE samples) for C_{16} FA, C_{18} FA, C_{20} FA, and C_{22} FA were in a range between 0.45 ± 0.04 μg/g (C_{18} FA) TLE and 1.36 ± 0.09 μg/g TLE (C_{16} FA) (Fig. 6C).

3.2. Automated SPE (aSPE)

Five blank columns were produced during each of the three replicate runs. Compounds were below detection in all of the 15 blanks.

3.2.1. Automated SPE Fraction 1

The F1 fraction of the automated SPE ($F1_{aSPE}$) samples contained the *n*-alkanes *n*-C_{25}, *n*-C_{27}, *n*-C_{29}, *n*-C_{31} and *n*-C_{33} (Fig. 4D, E, F) in a concentration range between 0.14 ± 0.00 μg/g (mean ± SE) to 0.87 ± 0.01 μg/g. The *n*-alkane with the lowest concentrations (from all identified *n*-alkanes) in all samples was *n*-C_{33}, whereas *n*-C_{29} had the highest concentration (Fig. 5A). Similar to the mSPE samples, aSPE sample concentrations varied for different TLE sample weights. $F1_{(15)aSPE}$ contained the highest concentrations of *n*-alkanes (range from 0.17 ± 0.00 μg/g TLE to 0.87 ± 0.01 μg/g TLE) (Fig. 5A, Table 1). The *n*-alkane concentrations for the samples $F1_{(20)aSPE}$, $F1_{(25)aSPE}$ and $F1_{(30)aSPE}$ were in a range from 0.14 ± 0.00 μg/g TLE to 0.75 ± 0.02 μg/g TLE but always within the respective ranges of the SE (Fig. 5A, Table 1). The overall mean concentration for *n*-C_{25} was 0.20 ± 0.01 μg/g TLE, for *n*-C_{27} 0.57 ± 0.02 μg/g TLE, for *n*-C_{29} 0.77 ± 0.03 μg/g TLE, for *n*-C_{31} 0.44 ± 0.02 μg/g TLE and for *n*-C_{33} 0.15 ± 0.01 μg/g TLE (Fig. 6A). In contrast to the $F1_{mSPE}$ runs all $F1_{aSPE}$ replicates contained 1,2-benzacenaphthene and pyrene. The highest concentration of 1,2-benzacenaphthene and pyrene was found in $F1_{(15)aSPE}$

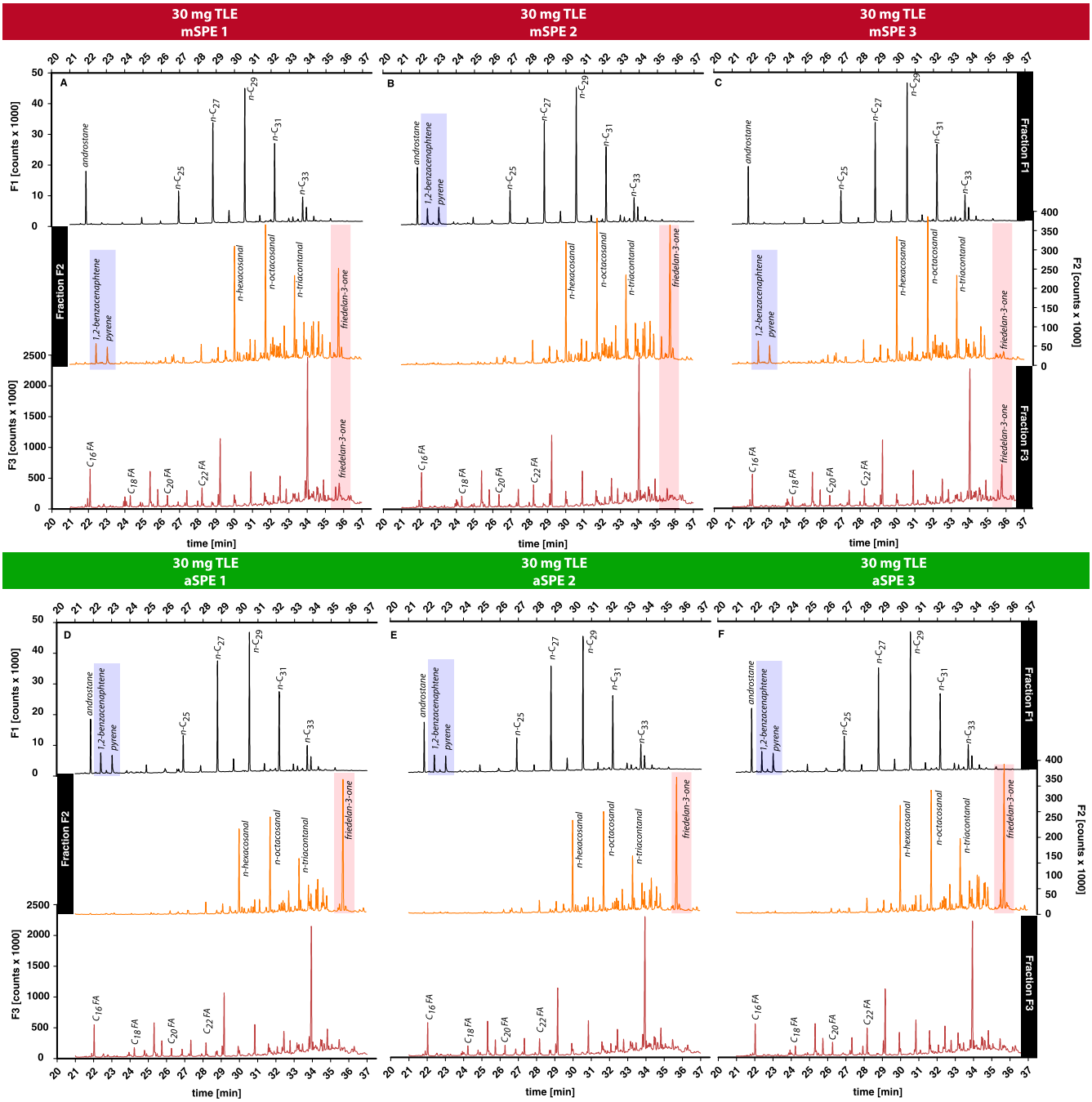

Fig. 4. Chromatograms of aSPE and mSPE samples. (A), (B) and (C) showing chromatograms of the three replicas of fractions $F1_{(30)}$mSPE, $F2_{(30)}$mSPE and $F3_{(30)}$mSPE. (D), (E) and (F) showing chromatograms of the three replicas of fractions $F1_{(30)}$aSPE, $F2_{(30)}$aSPE, and $F3_{(30)}$aSPE. Boxes mark compounds which are indicative of separation quality.

(0.16 ± 0.02 μg/g TLE and 0.17 ± 0.02 μg/g TLE). The samples $F1_{(20)aSPE}$,$F1_{(25)aSPE}$ and $F1_{(30)aSPE}$ contained mean concentrations between 0.09 ± 0.07 μg/g TLE and 0.10 ± 0.13 μg/g TLE of 1,2-benzacenaphthene and 0.10 ± 0.06 μg/g TLE and 0.11 ± 0.10 μg/g TLE of pyrene (Fig. 4D, E, F). Those variations were within the SE of the replicate measurements.

δ^2H values of n-C_{25} from $F1_{(15)aSPE}$,$F1_{(20)aSPE}$, $F1_{(25)aSPE}$ and $F1_{(30)aSPE}$ displayed mean values between −157.3 ± 1.1‰ and −158.7 ± 1.6‰. For n-C_{27}, n-C_{29}, n-C_{31} and n-C_{33} the mean values are between −168.2 ± 0.6‰ and −169.3 ± 0.5‰, −162.3 ± 0.5‰ and −164.1 ± 0.7‰, −172.4 ± 0.5‰ and −173.3 ± 0.4‰, −159.3 ± 0.8‰ and −161.2 ± 0.6‰ (Table 2). Similar to mSPE samples, no systematic difference was observed for δ^2H values among the different TLE concentrations. The specific n-alkane δ^2H values (averaged over all TLE amounts samples) for n-C_{25}, n-C_{27}, n-C_{29}, n-C_{31}, and n-C_{33} were −157.7 ± 0.6‰, −168.6 ± 0.3‰, −163.1 ± 0.3‰, −172.8 ± 0.3‰ and −160.1 ± 0.4‰.

3.2.2. Fraction 2

The second aSPE fraction contained several aldehydes and ketones, although not all were baseline separated in the GC–MS chromatogram. For comparison with mSPE, we quantified the same three aldehydes (n-hexacosanal, n-octacosanal and n-triacontanal) and the ketone friedelan-3-one (Fig. 4D, E, F) as present in $F2_{mSPE}$. Similarly, the concentration of analyzed compounds in $F2_{aSPE}$ showed variations for different TLE sample weights. $F2_{(15)}$

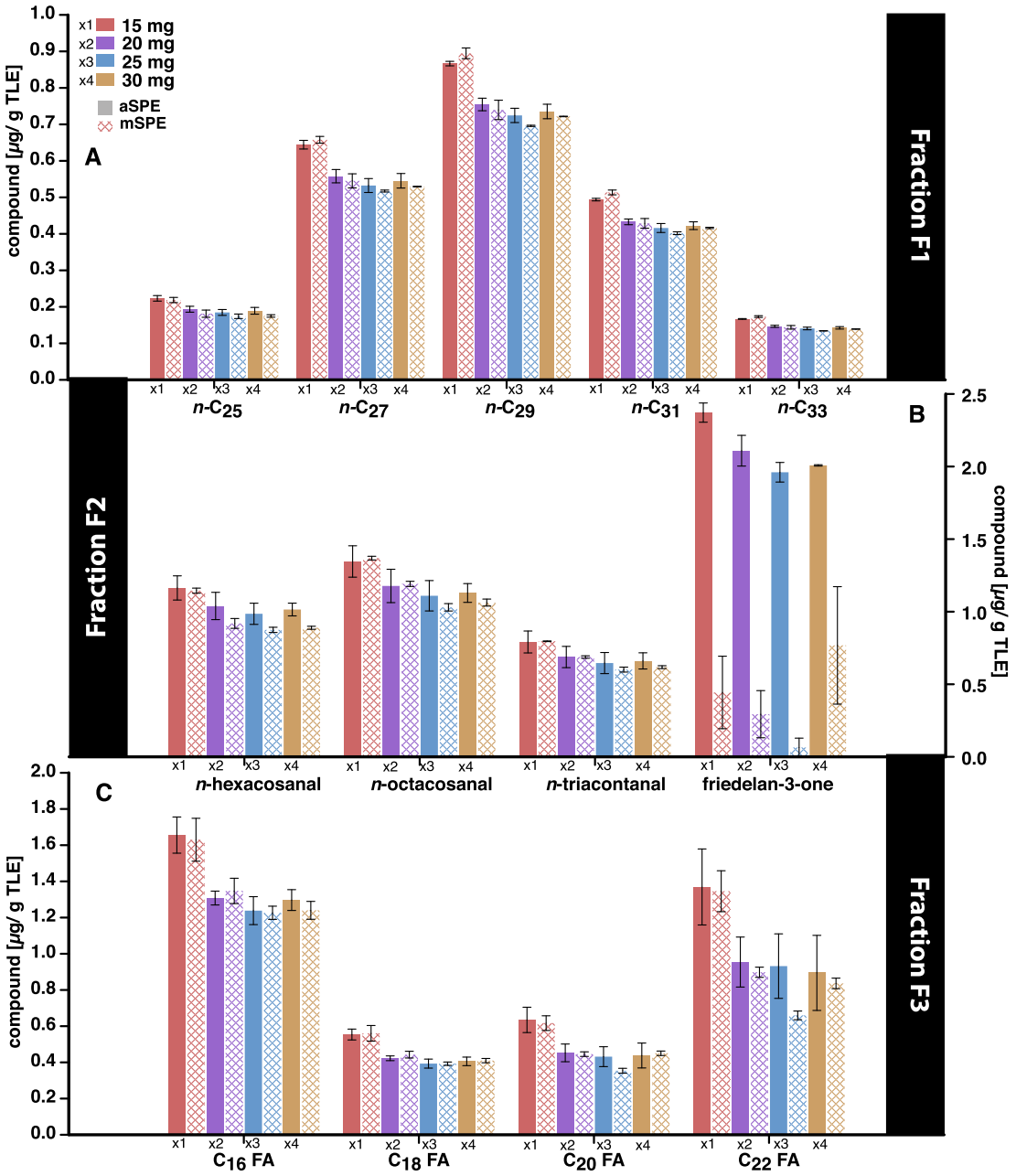

Fig. 5. Comparison of compound-specific amounts between aSPE and mSPE samples (normalized to TLE amounts). Error bars displaying the calculated standard error of the mean. (A) shows the respective mean amounts of *n*-alkanes of aSPE (full colored) and mSPE (half colored) separated samples. (B) displays the respective mean amounts of analyzed aldehydes and ketone of aSPE (full colored) and mSPE (half colored) separated samples. (C) shows the respective mean amounts of analyzed fatty acids of aSPE (full colored) and mSPE (half colored) separated samples.

$_{aSPE}$ contained the highest concentration of *n*-hexacosanal, *n*-octacosanal, *n*-triacontanal and friedelan-3-one (1.16 ± 0.08 µg/g TLE, 1.35 ± 0.11 µg/g TLE, 0.79 ± 0.08 µg/g TLE and 2.37 ± 0.07 µg/g TLE) (Fig. 5B, Table 1). For $F2_{(20)aSPE}$, $F2_{(25)aSPE}$, and $F2_{(30)aSPE}$ *n*-hexacosanal, *n*-octacosanal and *n*-triacontanal showed concentrations in a range between 0.65 ± 0.07 µg/g TLE and 1.18 ± 0.11 µg/g TLE whereas the concentration of friedelan-3-one varied between 1.96 ± 0.07 µg/g TLE and 2.11 ± 0.11 µg/g TLE. The differences in compound concentration between $F2_{(20)aSPE}$, $F2_{(25)aSPE}$ and $F2_{(30)aSPE}$ were within the respective range of the SE (Fig. 5B, Table 1). In the $F2_{aSPE}$ measurements, we observed no significant differences within the mean SE of *n*-hexacosanal, *n*-octacosanal and *n*-triacontanal (0.08 µg/g TLE) and friedelan-3-one (0.06 µg/g TLE). The respective mean concentrations for *n*-hexacosanal, *n*-octacosanal and *n*-triacontanal were 1.05 ± 0.04 µg/g TLE, 1.19 ± 0.05 µg/g TLE and 0.70 ± 0.03 µg/g TLE and was 2.11 ± 0.09 µg/g TLE for friedelan-3-one (Fig. 6B).

3.2.3. Fraction 3

The third aSPE fraction ($F3_{aSPE}$) contained (similar to mSPE results) C_{16} FA, C_{18} FA, C_{20} FA and C_{22} FA (Fig. 4D, E, F) with concentration differences for different TLE sample weights. The highest concentration of C_{16} FA, C_{18} FA, C_{20} FA and C_{22} FA were measured in $F3_{(15)aSPE}$ (1.66 ± 0.10 µg/g TLE, 0.55 ± 0.03 µg/g TLE, 0.63 ± 0.07 µg/g TLE and 1.37 ± 0.21 µg/g TLE) (Fig. 5C, Table 1). In $F3_{(20)aSPE}$, $F3_{(25)aSPE}$ and $F3_{(30)aSPE}$ the identified FA's ranged in concentrations between 0.39 ± 0.02 µg/g TLE and 1.31 ± 0.04 µg/g TLE. These variations were within the range of the SE (Fig. 5C, Table 1).

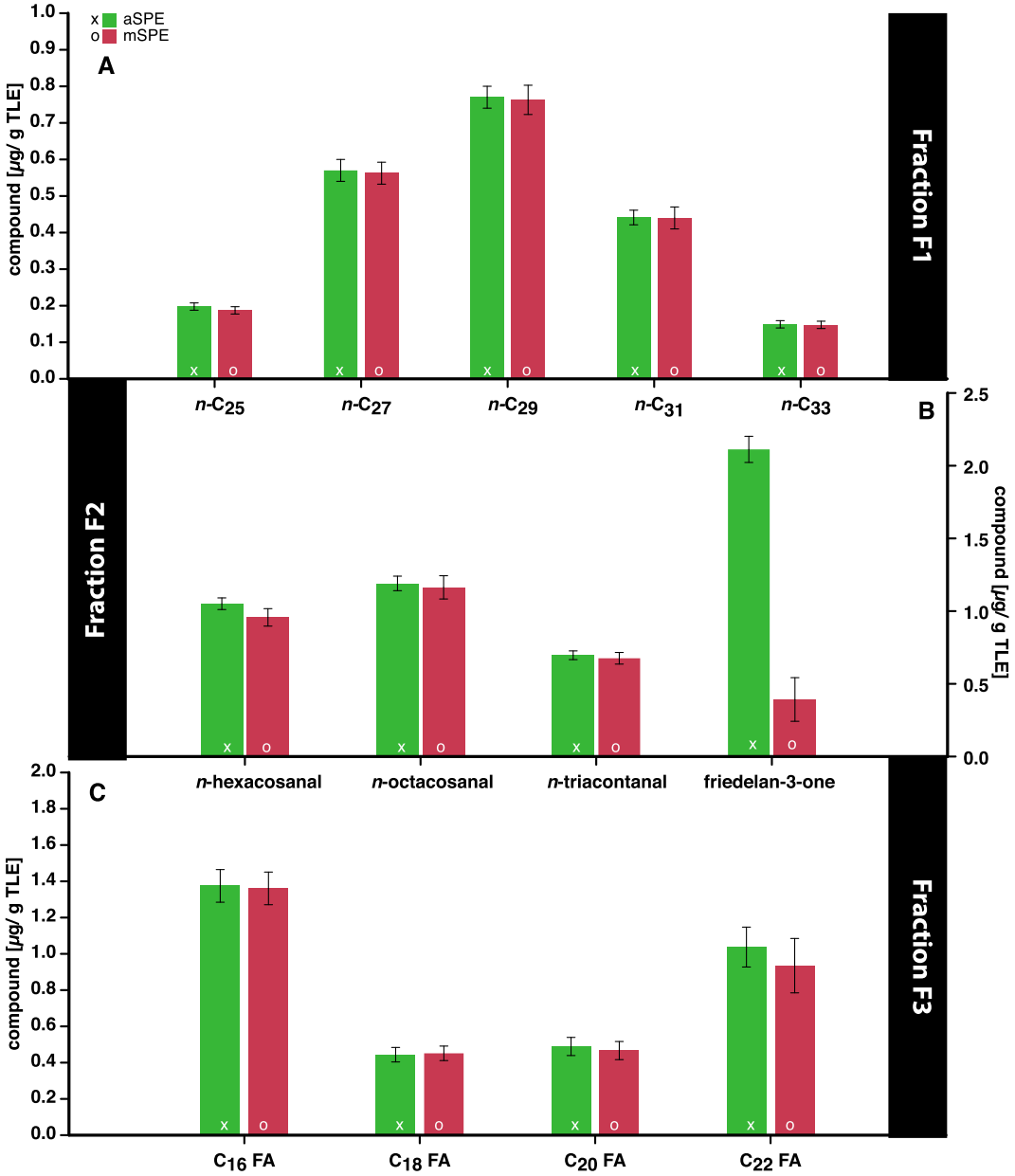

Fig. 6. Comparison of normalized mean compound-specific amounts (over all processed samples) between aSPE and mSPE. Error bars show the calculated standard error of the mean. (A) displays the mean compound concentration for *n*-alkanes (green (x) = aSPE, red (o) = mSPE). (B) Shows the mean compound concentrations for aldehydes and ketone (green (x) = aSPE, red (o) = mSPE). (C) Displays the mean compound concentration for fatty acids (green (x) = aSPE, red (o) = mSPE). (For interpretation of the references to colour in this figure legend, the reader is referred to the web version of this article.)

The respective mean concentrations in $F3_{aSPE}$ for C_{16} FA, C_{18} FA, C_{20} FA and C_{22} FA were in a range between 0.44 ± 0.04 µg/g TLE and 1.37 ± 0.09 µg/g TLE (Fig. 6C).

4. Discussion

The comparison of the classical mSPE with a fully automated system (aSPE) showed general similarities but also distinct differences in separation quality, reproducibility and time demand. All compounds detected in mSPE fractions were also detected in aSPE fractions, suggesting similar separation capabilities and the general comparability of both methods. The observed patterns of compound distributions were comparable and the *n*-alkane average chain length (ACL) index was identical for mSPE and aSPE samples (28.8). Overall lipid concentrations were comparable (Fig. 5), except for friedelan-3-one eluting in F2 and/or F3 and 1,2-benzacenaphthene and pyrene eluting in F1 or F2 (Fig. 4), indicating quality differences between both methods.

4.1. Quality of automated vs manual SPE separations

The qualitative evaluation of all SPE fractions showed significant differences between aSPE and mSPE results. For example, in all $F1_{aSPE}$ samples, we detected 1,2-benzacenaphthene and pyrene (Fig. 4D, E, F), polycyclic aromatic hydrocarbons (PAHs) produced during combustion processes and probably transported to the sampling location by wind or car traffic. In the mSPE fractions, however, these compounds (Fig. 4A, B, C) were only found in four out of 12 mSPE F1 fractions. In the remaining 8 mSPE replicates these unsaturated compounds were detected in the F2 fraction. Similarly,

friedelan-3-one was detected in variable amounts in the mSPE F2 and F3 fraction (Figs. 4, 5), indicating inconsistent separation into the two more polar fractions. On the contrary, friedelan-3-one eluted exclusively and in consistent concentrations in the F2 fraction of the aSPE, providing evidence for the superior reproducibility of aSPE separations. Likely, inhomogeneities in the (manually packed) silica gel columns are better compensated by the controlled constant solvent flow of the aSPE compared to primary gravity-driven solvent flow in manual SPE. In summary, while differences in *n*-alkane distributions were not detected between both methods, aSPE did show a better reproducibility concerning the more polar compounds friedelan-3-one, 1,2-benzacenaphthene, and pyrene.

4.2. Quantitative differences between aSPE and mSPE

We observed only small differences in compound concentrations in a direct comparison between aSPE and mSPE, most of which were not larger than the standard error of the replicate extractions. However, for both methods, we detected some variations in compound output as a function of initial TLE weights.

When comparing the *n*-alkane concentrations (TLE normalized amounts) of $F1_{aSPE}$ and $F1_{mSPE}$ we observed a small but significantly higher concentration (p-value less than 0.05, confidence interval always: 95%) for the 15 mg TLE sample than for all other extracts (Fig. 5A). The $F1_{(15)mSPE}$ fraction contained 0.10 ± 0.02 µg/g TLE and $F1_{(15)aSPE}$ 0.07 ± 0.02 µg/g TLE more *n*-alkanes (summed concentration of all quantified *n*-alkanes, mean value of three replicates respectively) than the 20 mg, 25 mg, and 30 mg TLE samples. For the 20 mg, 25 mg and 30 mg TLE samples the quantitative differences in $F1_{mSPE}$ and $F1_{aSPE}$ were within the respective SEs and therefore not significant (p-value > 0.05). Similar observations were made for the $F2_{(15)mSPE}$ but not the $F2_{(15)aSPE}$ fraction for quantified aldehydes, and the $F3_{(15)mSPE}$ and $F3_{(15)aSPE}$ fractions, which all showed significantly higher concentrations than the higher TLE weight samples.

The slightly, but significant, higher concentration found in the lowest TLE weights fractions is surprising and we can only speculate about the cause for this observation. Possibly, 15 mg constitutes an optimal amount of TLE for the amount of silica gel used, i.e. an optimal solid phase/TLE ratio. Higher TLE amounts may lead to a decreased separation efficiency caused by sample–matrix interactions or column overload. In the latter case, we would expect to detect apolar compounds in the more polar F2 or F3 fractions, which we did not. However, the overall concentration difference is small and it is conceivable that any apolar compounds eluting in F2 or F3 were below the GC–MS/FID's detection limit. Since concentration differences between $F1_{mSPE}$ and $F1_{aSPE}$ fractions were not significant (p-value always > 0.05) (Fig. 5A) this is not a disadvantage of the aSPE rather a general SPE phenomenon.

For F2 and the F3 fraction of the aSPE we observed × 4 and × 2 higher SEs compared to their mSPE counterparts. For both $F1_{aSPE}$ and $F1_{mSPE}$ this is possibly related to insufficient repeated automatic rinsing of the sample vial before the start of elution of fraction F2 and F3. During mSPE this step can be performed more accurately. However, apart from the increased SE during $F2_{aSPE}$ there were no significant differences in concentrations between $F2_{aSPE}$ and $F2_{mSPE}$ (Figs. 5B and 6B).

We, however, observed significant differences in separation quality and reproducibility between $F2_{aSPE}$ and $F2_{mSPE}$ with signif-

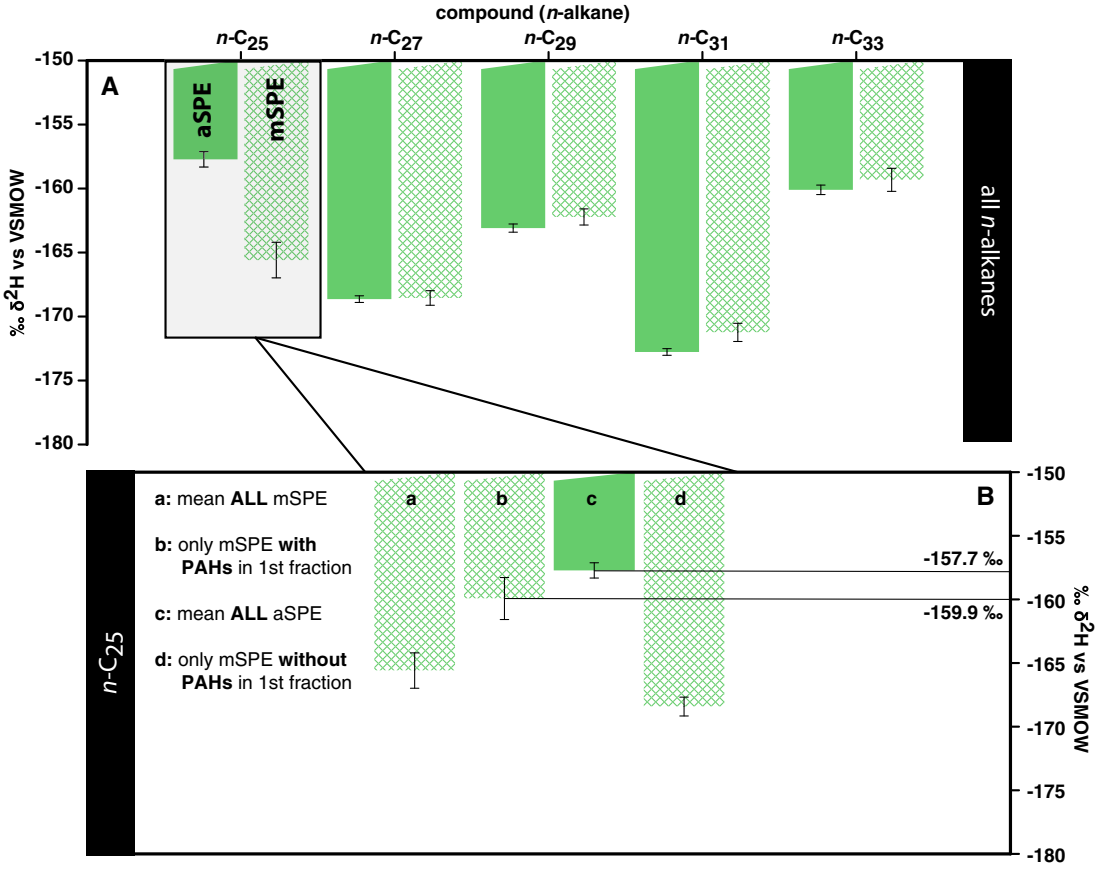

Fig. 7. Comparison of compound-specific mean δ^2H values between aSPE and mSPE. Error bars displaying the calculated standard error of the mean. (A) Shows the mean compound-specific δ^2H values for all analyzed *n*-alkanes (full colored = aSPE samples, half colored = mSPE samples). (B) Displays the mean compound-specific δ^2H values for $n\text{-}C_{25}$ (full colored = aSPE samples, half colored = mSPE samples) separated by the occurrence of PAHs within the samples.

icantly lower amounts of friedelan-3-one detected in the $F2_{mSPE}$ fraction (Fig. 5B), which suggests a superior separation quality and reproducibility of these polar and unsaturated compounds in aSPE (Fig. 6B).

4.3. Compound-specific δ^2H results

Stable hydrogen isotope ratios (δ^2H values) of n-C_{25}, n-C_{27}, n-C_{29}, n-C_{31}, and n-C_{33} from the F1 fractions of mSPE and aSPE were identical within the SE for n-C_{27}, n-C_{29}, n-C_{31}, and n-C_{33} but were about 8‰ more positive for n-C_{25} from the $F1_{aSPE}$ (-157.7 ± 0.6‰) compared to the $F1_{mSPE}$ sample (-165.6 ± 1.4‰.). This difference is significantly above analytical accuracy (Fig. 7A, B). Interestingly, n-C_{25} δ^2H values from $F1_{mSPE}$ fractions containing 1,2-benzacenaphthene and pyrene (n = 4) were characterized with -159.9 ± 1.6‰ and were also more positive than the mean of all $F1_{mSPE}$ samples. As such, the n-C_{25} δ^2H values for both aSPE and mSPE were identical if 1,2-benzacenaphthene and pyrene were present within the F1 fraction (Fig. 7B). Since 1,2-benzacenaphthene and pyrene are produced during combustion processes they are expected to be deuterium-enriched, with more positive δ^2H ratios (between -70‰ and -95‰) compared to long-chain n-alkanes (Liu et al., 2006; Sachse et al., 2006; Sachse et al., 2012). Since the peaks of both PAHs, as well as the peak of n-C_{25}, were baseline separated from adjacent compounds, coelution can be ruled out as a factor. Rather, we suggest the more positive δ^2H values of n-C_{25} when PAHs were present in the same fraction implies a possible memory effect on the δ^2H value of the first eluting n-C_{25}, but not on the later eluting n-alkanes, as their δ^2H values were almost identical within the SE among all other fractions. Such memory effects have been observed in GC–TC-IRMS systems and are related to the working principles of current gas chromatography and coupled stable isotope mass spectrometers, likely due to adsorption of pyrolysis products in the high-temperature reactor (Wang and Sessions, 2008). The magnitude of a memory effect varies as a function of absolute differences in isotope values between peaks. The distance of the respective peaks, relative concentrations of those peaks (Wang and Sessions, 2008) as well as reactor age and other analytical conditions. Interestingly, δ^2H values of n-alkanes are not affected by the proposed PAH memory effect (n-C_{27}, n-C_{29}, n-C_{31}, and n-C_{33}) the mean SE (0.30 ± 0.02‰) was 2.3 times lower for aSPE samples compared to mSPE samples (0.70 ± 0.06‰) (Fig. 7A) (Fig. 8A, B). This provides another example of the better separation quality of aSPE samples. Possibly small variations in sample background, which are not adequately separated in mSPE, can lead to slightly different δ^2H values. The observed lower SEs of aSPE δ^2H values suggest superior reproducibility during replicate runs and therefore a clear advantage of the aSPE method.

4.4. Procedure duration

Automated SPE in our three-fraction setup runs unattended with 9 subsequent samples analyzed in less than 14 h (ca. 92 min/sample), leaving the user to perform other work or to improve work-life balance. Also, aSPE separations can be run unattended overnight. Set up time, i.e. column and workplace preparation, including preparation of solvent and chemicals is almost

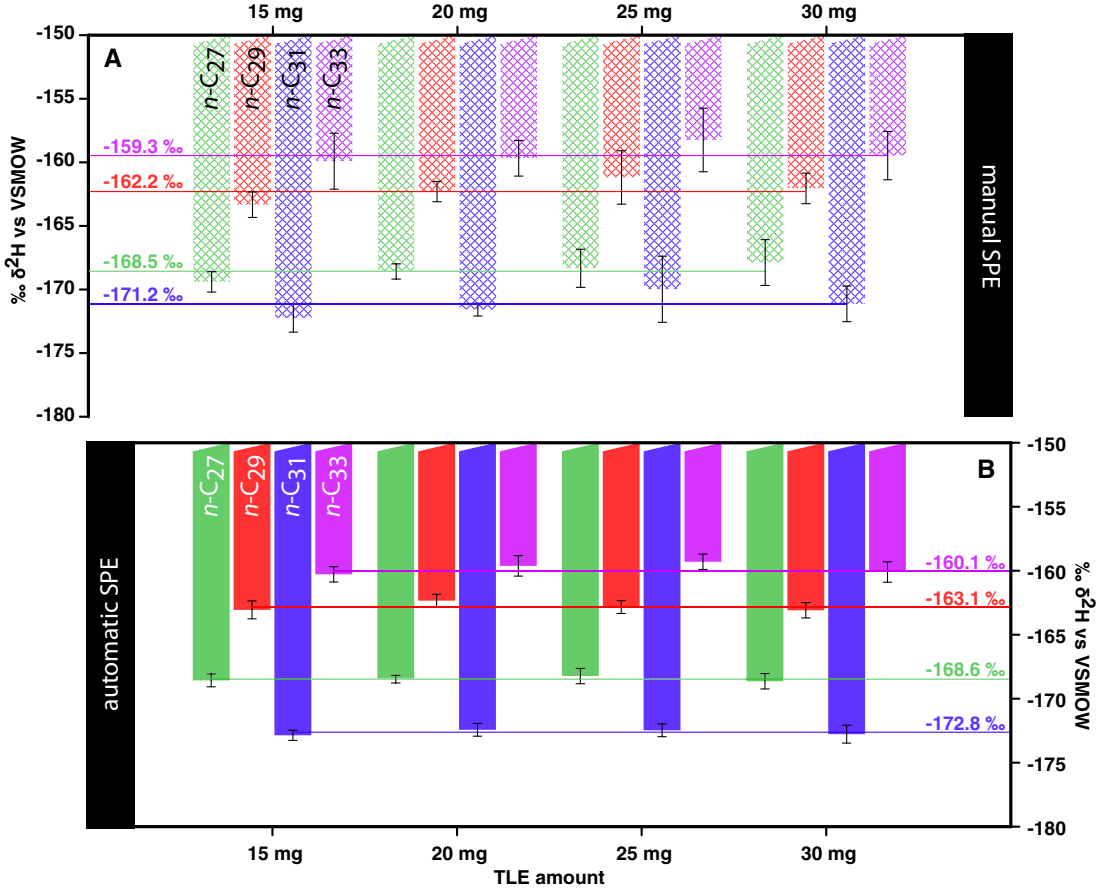

Fig. 8. Comparison of compound-specific mean δ^2H values between aSPE and mSPE for different TLE weights. Error bars showing the calculated standard error of the mean. (A) Shows the compound-specific mean δ^2H values for different TLE weights from mSPE samples. (B) Displays the compound-specific mean δ^2H values for different TLE weights from aSPE samples.

identical for aSPE and mSPE. The manual separation procedure of four samples into three fractions (done by a trained and experienced technician) can be completed in one hour but requires constant personnel attendance during the procedure.

5. Conclusions

We present a new fully automated solid phase (aSPE) extraction-based purification procedure for lipid biomarkers using the Gilson ASPEC GX-271. We compare its separation quality, reproducibility, quantitative aspects and efficiency to a classical manual lipid purification procedure (mSPE) commonly used in organic geochemical laboratories. Both methods deliver high-quality separation, but we find significant advantages for aSPE in separation quality, reproducibility and use of time. We found a significantly improved separation quality for aSPE over mSPE, with a consistent and reproducible separation of compounds into the three fractions. In contrast, during mSPE runs some compounds (like 1,2-benzacenaphthene, pyrene and friedelan-3-one) eluted into different fractions during replicate separations. Additionally, compound-specific (*n*-alkane) δ^2H measurements on those samples showed significantly lower standard errors of aSPE samples, likely due to a better compound separation. We found no significant differences in the distribution or concentration of lipids between aSPE and mSPE.

In general, both methods showed slightly higher compound concentrations for lower concentrations of TLEs, probably related to an overload of the SPE column for sample amounts $\geq$ 20 mg. The efficiency between the manual and automated approach, which can be expressed in time per sample, can only be compared with limitations. Manual SPE allows the processing of several samples in parallel while aSPE (in our setup) processes only one sample at a time. Therefore, for mSPE the general output of samples per time unit is higher but this is compensated by the fact that aSPE can be performed unattended (for example overnight). The general weighting of these aspects is surely individual and application-specific, but the significantly better separation quality, the resulting lower standard error of δ^2H values of aSPE separated compounds, as well as reproducibility, the unattended and simple operation of an aSPE make it attractive for applications and labs where high lipid biomarker separation output is needed (i.e. temporal high-resolution lipid biomarker studies).

Declaration of Competing Interest

The authors declare that they have no known competing financial interests or personal relationships that could have appeared to influence the work reported in this paper.

Acknowledgements

This study was supported by an ERC Consolidator grant (STEEP-clim, Grant agreement No. 647035) to Dirk Sachse. We thank the reviewers for their helpful comments.

Associate Editor—**Elizabeth Minor**

References

Atwood, A.R., Sachs, J.P., 2012. Purification of dinosterol from complex mixtures of sedimentary lipids for hydrogen isotope analysis. Organic Geochemistry 48, 37–46.

Curtin, L., D'Andrea, W.J., Balascio, N., Pugsley, G., de Wet, G., Bradley, R., 2019. Holocene and last interglacial climate of the Faroe Islands from sedimentary plant wax hydrogen and carbon isotopes. Quaternary Science Reviews 223, 105930.

Feakins, S.J., Wu, M.S., Ponton, C., Tierney, J.E., 2019. Biomarkers reveal abrupt switches in hydroclimate during the last glacial in southern California. Earth and Planetary Science Letters 515, 164–172.

Gamarra, B., Sachse, D., Kahmen, A., 2016. Effects of leaf water evaporative ^{2}H-enrichment and biosynthetic fractionation on leaf wax *n*-alkane δ^2H values in C3 and C4 grasses. Plant, Cell & Environment 39, 2390–2403.

Gilson.com, 2019. https://de.gilson.com/DEDE/gx-271-aspec-dual-4260-with-z-drive.html.

Hoffmann, B., Kahmen, A., Cernusak, L.A., Arndt, S.K., Sachse, D., 2013. Abundance and distribution of leaf wax *n*-alkanes in leaves of Acacia and Eucalyptus trees along a strong humidity gradient in northern Australia. Organic Geochemistry 62, 62–67.

Ladd, S.N., Sachs, J.P., 2012. Inverse relationship between salinity and *n*-alkane δD values in the mangrove Avicennia marina. Organic Geochemistry 48, 25–36.

Liu, W.G., Yang, H., Li, L.W., 2006. Hydrogen isotopic compositions of *n*-alkanes from terrestrial plants correlate with their ecological life forms. Oecologia 150, 330–338.

McInerney, F.A., Helliker, B.R., Freeman, K.H., 2011. Hydrogen isotope ratios of leaf wax *n*-alkanes in grasses are insensitive to transpiration. Geochimica et Cosmochimica Acta 75, 541–554.

Nelson, D.B., Knohl, A., Sachse, D., Schefuß, E., Kahmen, A., 2017. Sources and abundances of leaf waxes in aerosols in central Europe. Geochimica et Cosmochimica Acta 198, 299–314.

Poole, C.F., 2003. New trends in solid-phase extraction. TrAC Trends in Analytical Chemistry 22, 362–373.

Rach, O., Brauer, A., Wilkes, H., Sachse, D., 2014. Delayed hydrological response to Greenland cooling at the onset of the Younger Dryas in western Europe. Nature Geoscience 7, 109–112.

Radke, M., Willsch, H., Welte, D.H., 1980. Preparative hydrocarbon group type determination by automated medium pressure liquid chromatography. Analytical Chemistry 52, 406–411.

Romero, I.C., Feakins, S.J., 2011. Spatial gradients in plant leaf wax D/H across a coastal salt marsh in southern California. Organic Geochemistry 42, 618–629.

Sachse, D., Billault, I., Bowen, G.J., Chikaraishi, Y., Dawson, T.E., Feakins, S.J., Freeman, K.H., Magill, C.R., McInerney, F.A., van der Meer, M.T.J., Polissar, P., Robins, R.J., Sachs, J.P., Schmidt, H.-L., Sessions, A.L., White, J.W.C., West, J.B., Kahmen, A., 2012. Molecular paleohydrology: Interpreting the hydrogen-isotopic composition of lipid biomarkers from photosynthesizing organisms. Annual Review of Earth and Planetary Sciences 40, 221–249.

Sachse, D., Radke, J., Gleixner, G., 2006. δD values of individual *n*-alkanes from terrestrial plants along a climatic gradient – Implications for the sedimentary biomarker record. Organic Geochemistry 37, 469–483.

Sessions, A.L., 2006. Seasonal changes in D/H fractionation accompanying lipid biosynthesis in *Spartina alterniflora*. Geochimica et Cosmochimica Acta 70, 2153–2162.

Stout, P.R., Horn, C.K., Klette, K.L., 2001. Solid-phase extraction and GC–MS analysis of THC-COOH method optimized for a high-throughput forensic drug-testing laboratory. Journal of Analytical Toxicology 25, 550–554.

Telepchak, M.J., August, T.F., Chaney, G.C., 2004. Forensic and Clinical Applications of Solid Phase Extraction. Humana Press, Totowa, NJ, USA.

Tierney, J.E., Oppo, D.W., Rosenthal, Y., Russell, J.M., Linsley, B.K., 2010. Coordinated hydrological regimes in the Indo-Pacific region during the past two millennia. Paleoceanography 25, PA1102.

Vogts, A., Moossen, H., Rommerskirchen, F., Rullkötter, J., 2009. Distribution patterns and stable carbon isotopic composition of alkanes and alkan-1-ols from plant waxes of African rain forest and savanna C_3 species. Organic Geochemistry 40, 1037–1054.

Wang, Y., Sessions, A.L., 2008. Memory effects in compound-specific D/H analysis by gas chromatography/pyrolysis/isotope-ratio mass spectrometry. Analytical Chemistry 80, 9162–9170.

Wohlfarth, B., Luoto, T.P., Muschitiello, F., Väliranta, M., Björck, S., Davies, S.M., Kylander, M., Ljung, K., Reimer, P.J., Smittenberg, R.H., 2018. Climate and environment in southwest Sweden 15.5–11.3 cal. ka BP. Boreas 47, 687–710.

Xu, L., Lee, H.K., 2008. Novel approach to microwave-assisted extraction and micro-solid-phase extraction from soil using graphite fibers as sorbent. Journal of Chromatography A 1192, 203–207.

Zelles, L., Bai, Q.Y., 1993. Fractionation of fatty acids derived from soil lipids by solid phase extraction and their quantitative analysis by GC-MS. Soil Biology and Biochemistry 25, 495–507.

Zhou, J., Wu, J., Ma, L., Abuduwaili, J., 2019. Late Quaternary environmental change record in biomarker lipid compositions of Lake Ebinur sediments, northwestern China. International Journal of Earth Sciences 108, 2361–2371.